Proton Nuclear Magnetic Resonance Study of a Self-Complementary Decadeoxyribonucleotide, C-C-A-A-G-C-T-T-G-G†

L.-S. Kan,* D. M. Cheng, K. Jayaraman, E. E. Leutzinger, P. S. Miller, and P. O. P. Ts'o

ABSTRACT: A short DNA helix, d-(C-C-A-A-G-C-T-T-G-G)$_2$, has been thoroughly investigated by ^{1}H NMR spectroscopy. All 17 nonexchangeable base proton resonances have been assigned by the aid of the assigned ^{1}H NMR spectra of two half-decamer molecules (C-C-A-A-G and C-T-T-G-G) [Cheng, D. M., Kan, L.-S., Leutzinger, E. E., Jayaraman, K., Miller, P. S., & Ts'o, P. O. P. (1982) *Biochemistry 21*, 621] and their equimolar mixture at high temperature. The five NH–N hydrogen-bonded resonances were assigned by a thermal perturbation procedure as well as by nuclear Overhauser effects (NOE) from the already assigned base protons. These assignment procedures can be adopted as a guide for the assignment of the base proton resonances in other short helices comprised of 6–15 nucleotidyl units. The assigned nonexchangeable proton resonances at high temperature were carefully followed to low temperature and gave sigmoid curves indicative of cooperative helix to coil transitions. The assignment of $H_{1'}$ proton resonances in the helical state was made from the assigned base proton resonances with the application of double resonance techniques and NOE experiments. The analysis of the sugar puckering conformation of this helix can be estimated from the well-resolved resonances of $H_{1'}$. All the nucleotidyl residues of the helix are predominantly in the $C_{2'}$-endo form within a range of graded variation of 66–87% starting from the terminal nucleotides to residues toward the center residue of the helix. Thus, the circular dichroism data [Miller, P. S., Cheng, D. M., Dreon, N., Jayaraman, K., Kan, L.-S., Leutzinger, E. E., Pulford, S. M., & Ts'o, P. O. P. (1980) *Biochemistry 19*, 4688] and the sugar conformational analyses strongly indicate that this short DNA helix assumes a conformation in aqueous solution similar to but not necessarily identical with the B form. The through-space magnetic field effects on the base protons and NH–N protons in the helices were calculated and compared with the observed values. This comparison indicates that for the base protons, application of both ring-current effects and atomic anisotropic effects is preferred but for the NH–N protons the application of ring-current effect alone is preferred over the application of both ring-current effects and atomic anisotropic effects. The usefulness of the polarization effect remains to be further evaluated. The computed values, derived from the best theoretical treatment cited above, do support the conclusion that this helix assumes a B conformation. With all the resonances of the base protons, $H_{1'}$ protons, and NH–N protons individually and reliably assigned, this stable decameric DNA helix can serve as an effective model system for the testing of NMR theory and application to nucleic acid research.

Short oligoribo- and oligodeoxyribonucleotide helices with defined sequences are excellent models for studies of RNA and DNA conformations. Three stable helices have been crystallized and studied by X-ray diffraction techniques (Wang et al., 1979; Crawford et al., 1980; Drew et al., 1980; Dickerson & Drew, 1981). These studies provide information on the conformation of these helices at the atomic level of resolution. The short helices can also be examined in solution by high-resolution NMR spectroscopy. Correlation of nucleic acid conformation in the crystalline and solution states can be made by comparing the X-ray and NMR results. While these helices are sufficiently short to yield X-ray diffraction data and NMR signals for high-resolution investigation, they are long enough for studies on drug–nucleic acid helix interaction [for RNA helices, see Bubienko et al. (1981), Arter et al. (1974), Borer et al. (1975), Hughes et al. (1978), Romaniuk et al. (1978a,b 1979), and Alkema et al. (1981); for DNA, see Cross & Crothers (1971) and Patel and co-workers work, for example, Patel (1979), Patel et al. (1982a–d), and Early et al. (1978); for DNA–RNA hybrid, see Pardi et al. (1981)] or enzyme–nucleic acid interactions (Miller et al., 1982).

Recently, we described the synthesis and preliminary characterization of a self-complementary decadeoxyribonucleotide, d-CCAAGCTTGG (Miller et al., 1980). This decamer forms a stable helix at room temperature and medium ionic strength as indicated by ultraviolet (UV), circular dichroism (CD), and NMR studies. The conformation of this helix in aqueous buffer most likely belongs to the B family as indicated by its CD spectrum. The sequence of the decamer helix contains recognition sites for *Alu*I (-A-G-C-T-), *Hin*dIII (-A-A-G-C-T-T-), and *Hsu*I (Scheller et al., 1977) restriction endonucleases.

In this paper, we report in detail the ^{1}H NMR assignments of all the nonexchangeable base proton, $H_{1'}$ proton, and NH–N hydrogen-bonded proton resonances of the decamer. This information has been used to study the mode of melting of the decamer helix. Analysis of the $H_{1'}$ sugar proton region provides information on the overall sugar puckering of the decamer backbone.

All the nucleotidyl residues of the helix are predominantly in the $C_{2'}$-endo form, with a graded variation of 66–87% starting from the terminal residues toward the center of the helix. The chemical shifts of the base proton in the monomeric units and the chemical shifts of the same proton in the decamer helix were measured. The resulting changes in chemical shift are compared with those expected for a helix in the A, A′, or B conformation based on theoretical calculations. This study indicates that this extensively characterized helix can serve as an effective model for the testing of NMR theory and application to nucleic acid research.

Experimental Procedures

The chemical synthesis and enzymatic characterization of the decadeoxyribonucleotide d-C-C-A-A-G-C-T-T-G-G and

† From the Division of Biophysics, School of Hygiene and Public Health, The Johns Hopkins University, Baltimore, Maryland 21205. *Received July 6, 1982.* This work was supported in part by Grants CA-27111 (to L.-S.K.) and GM 16066 (to P.O.P.T.) from the National Institutes of Health as well as by Grant PCM 80-23320 (to P.O.P.T) from the National Science Foundation.

0006-2960/82/0421-6723$01.25/0

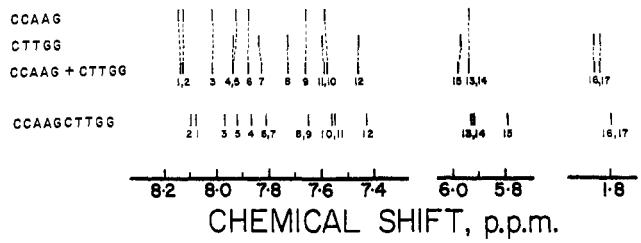

FIGURE 1: Assignment of the nonexchangeable base proton resonances of d-C^1-C^2-A^3-A^4-G^5-C^6-T^7-T^8-G^9-G^{10} with the aid of its two half-fragments, d-C-C-A-A-G and d-C-T-T-G-G. The numbering system of peaks is the following: 1 = A^4-H_8; 2 = A^3-H_8; 3 = A^4-H_2; 4 = A^3-H_2; 5 = G^{10}-H_8; 6 = G^5-H_8; 7 = G^9-H_8; 8 = C^6-H_6; 9 = C^1-H_6; 10 = C^2-H_6; 11 = T^7-H_6; 12 = T^8-H_6; 13 = C^1-H_5; 14 = C^2-H_5; 15 = C^6-H_5; 16 = T^7-CH_3; 17 = T^8-CH_3.

its fragments have been published (Miller et al., 1980; Cheng et al., 1982a).

Four high-field NMR spectrometers were used in this study, a Bruker WM-300 (located at the JHU–Baltimore NMR Biomedical Research Center, The Johns Hopkins University, Baltimore, MD), a WH-360 (located at The Mid-Atlantic Regional Facility, University of Pennsylvania, Philadelphia, PA), a WM-500 (located at the California Institute of Technology, Pasadena, CA), and a 600-MHz NMR spectrometer (homemade, located at Carnegie-Mellon University, Pittsburgh, PA). The first three spectrometers are equipped with Fourier transform (FT) and variable temperature capabilities. The 600-MHz instrument was used in the mode of correlation spectroscopy. All chemical shifts were measured from sodium 4,4-dimethyl-4-silapentane-1-sulfonate (DSS). The digital resolution of each spectrum including the correlation spectroscopy is 0.4 Hz/point or better. The NH–N hydrogen-bonded proton resonances were obtained both by correlation spectroscopy (360 and 600 MHz) and by the Redfield 214 pulse sequence (360 MHz in a solvent contained 80% H_2O and 20% D_2O). The nuclear Overhauser effect (NOE) experiments of NH–N proton resonance experiments were performed on the 600-MHz spectrometer. In addition, the NOE experiments involving the assignment of all $H_{1'}$ proton resonances were performed on the Bruker WM-300. A microprogram was written to obtain the different free induction decays (FID's) of on- and off-resonance spectra directly. Thus, all signals except the irradiated and influenced signal (the one obtained by NOE) are cancelled (see Figure 10B). The irradiation time and power are carefully controlled to eliminate spin diffusion (Early & Kearns, 1980).

Results and Discussion

Assignments of the Base Proton Resonances. (*a*) *Nonexchangeable Base Proton* (*or C–H*) *Resonances.* The nonexchangeable base proton resonances of the decamer including H_2 and H_8 of two adenines, H_8 of three guanines, H_5 and H_6 of three cytosines, H_6, and the methyl groups of two thymines can be assigned with the aid of the spectra of the two half-molecule fragments d-C-C-A-A-G and d-C-T-T-G-G. The nonexchangeable base proton resonances of the two half-molecule fragments were assigned previously (Cheng et al., 1982a). The strategy is illustrated in Figure 1. The first and second rows show the assignments of the base proton resonances of the two pentamers (Cheng et al., 1982a). As expected, the signals from a 1:1 mixture of the two pentamers at high temperature (75 °C) (row 3) can be represented very closely by the sum of rows 1 and 2. Thus, the identities of the nonexchangeable base proton resonances in the mixture of the two pentamers can be readily determined (Figure 1).

Comparison between the resonances of the pentamer mixture (row 3) with the resonances in the same region from the decamer (row 4) allows assignment of the nonexchangeable base proton resonances of the decamer. The decamer and the mixture of pentamers have the same base composition and sequence. The only difference is the presence of a phosphodiester linkage between G^5 and C^6 in the decamer. The spectrum in row 4 is very similar to that in row 3, especially the proton resonances from C^1, C^2, A^3, A^4, T^8, G^9, and G^{10}, at high temperature. This is expected because these bases are away from G^5–C^6 region. Therefore, they can be given the same assignment as those in the mixture of pentamers. On the other hand, the resonance of H_8 of G^5 (signal 6) moves upfield slightly as compared to H_8 of G^5 in the pentamer (row 3) due to the proximity of C^6 in the decamer. This assignment is further confirmed by exchange of H_8 with deuterium. The H_6 resonance of C^6 (signal 8) also shifts slightly upfield. The resonance cannot be shifted downfield to the region of signals 4 to 5 because this resonance (signal 8) is a doublet. The H_5 resonance of C^6 (signal 15) is assigned to the doublet located upfield of the two doublets 13 and 14. The crossover of signal 15 in the decamer as compared to its position in the pentamer mixture is due to the shielding of this proton by the neighboring G^5 in the decamer. In effect, this C residue moves from the 3′ end of the pentamer to the center of the decamer. The magnitude of the upfield shift (0.2 ppm) can be justified by model studies and by theoretical calculation of the chemical shifts (Giessner-Prettre et al., 1981). In addition, this assignment is supported by the profile of chemical shift vs. temperature in the following section (Figure 6). It is interesting to note that the H_6 resonance (signal 11) and methyl resonance (signal 16) of T^7 are also shifted upfield in the decamer relative to similar resonances in the pentamer. This upfield shift can also be attributed to the shielding of T^7 by G^5 which has now been linked to C^6 in the decamer. The H_6 doublet from T^7 (signal 11) has a very small coupling constant, and the H_6 doublet for C^6 (signal 10) has a large coupling constant. Thus, this assignment is confirmed by the coupling constants.

In conclusion, all 17 nonexchangeable base proton resonances of the decadeoxynucleotide d-C^1-C^2-A^3-A^4-G^5-C^6-T^7-T^8-G^9-G^{10} can be assigned with confidence.

(*b*) *NH–N Hydrogen-Bonded Proton Resonances.* Usually the assignment of these resonances is achieved by thermal perturbation of the helix (or helical region of the molecule). This method has been used to successfully assign the NH–N resonances of many short helices and tRNAs. In making these assignments, we always made two assumptions: (1) melting of a helix or helical region always starts from the outside base pairs and proceeds toward the inside base pairs, and (2) the increase in line width accurately represents the melting of the base pairs. In a circular argument, the NH–N resonance so assigned was then used as evidence for the stability of the presumed base pair. In this paper, an independent method for assignment was adopted which is based on knowledge of previously assigned nonexchangeable base proton resonances.

The decamer helix has a 2-fold center of symmetry. Therefore, at low temperature (0 °C), only five NH–N hydrogen-bonded resonances are observed. Two resonances are located downfield >14 ppm) and are assigned to AT pairs. The other three resonances are located upfield (around 13 ppm) and are assigned to GC pairs. The assignment of these five resonances is verified by examining the effect of temperature on the line width of these resonances. The results are shown in Table I. The resonance located at 13.24 ppm

Table I: Chemical Shifts (in ppm) and Line Widths at Half-Height (in Hz) (in Parentheses) of NH–N Proton Resonances of d-C-C-A-A-G-C-T-T-G-G[a]

temp (°C)	A_4-T_7	A_3-T_8	C_1-G_{10}	C_2-G_9	G_5-C_6
0	14.23 (13.5)	14.15 (17.3)	13.24 (34.5)	13.03 (16.5)	12.84 (16.5)
5	14.20 (16.5)	14.12 (15.0)	13.23 (36.0)	13.01 (16.5)	12.80 (16.5)
10	14.17 (13.5)	14.10 (13.5)	(57.0)	12.99 (16.5)	12.82 (15.0)
15	14.15 (18.0)	14.08 (16.5)	(61.5)	12.98 (16.5)	12.81 (16.5)
20	14.11 (13.5)	14.06 (13.5)		12.96 (15.0)	12.79 (15.0)
30	14.06 (18.0)	14.02 (12.0)		12.94 (21.0)	12.78 (13.5)
35	14.01 (13.5)	13.99 (10.5)		12.90 (21.0)	12.75 (15.0)
40	13.96 (15.0)			12.87 (45.0)	12.74 (12.0)
45	13.94 (22.5)			(58.0)	12.73 (12.0)
50	13.92 (30.0)				12.71 (24.0)
53	13.90 (54.0)				12.75 (37.5)

[a] In 0.1 N NaCl, 10^{-4} M ethylenediaminetetraacetic acid, and 0.1 M phosphate buffer, pH 7, solution.

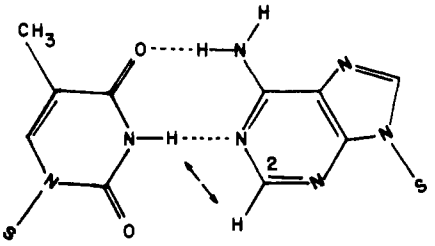

FIGURE 2: Watson–Crick hydrogen-binding scheme of an adenine-thymine base pair. The distance between the N_3-H of T to the C_2-H of A is calculated to be 2.84 Å (Kan et al., 1979). S represents the position of the $C_{1'}$ atom of the deoxyfuranose residue.

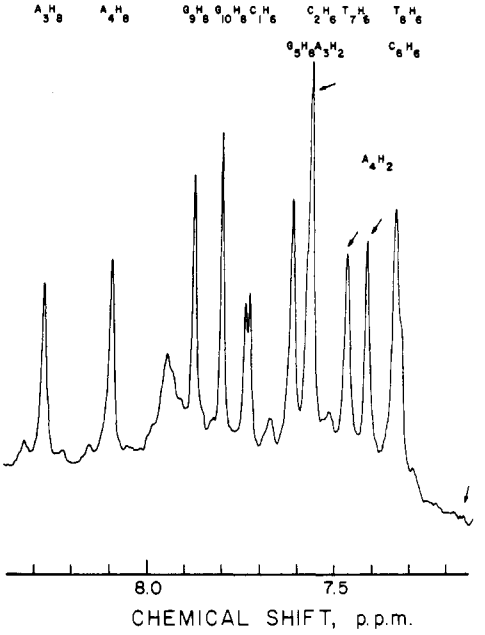

FIGURE 3: 600-MHz correlation spectrum of the base proton resonances of d-C-C-A-A-G-C-T-T-G-G in H_2O (contains 20% D_2O) solution. The ↓ symbol designates the frequency which has been irradiated. Since the spectrum was taken in H_2O as solvent, a broad unknown peak appears at ~7.95 ppm which may come from the exchangeable proton resonance(s). [The same spectrum which was taken in D_2O is shown in our previous paper (Miller et al., 1980).] Side bands, which are characteristic of the 600-MHz spectrometer at CMU, have also been shown.

(0–5 °C) broadens first when the temperature is raised to 10–15 °C and disappears at 20 °C. Therefore, this resonance is assigned to the two outermost base pairs, C^1·G^{10}. The resonance at 13.03 ppm (0–5 °C) broadens at 40 °C and begins to disappear at 45 °C. This resonance is thus assigned to the two external base pairs C^2·G^9. The two NH–N resonances from the AT base pairs are located close together (14.23 and 14.15 ppm). They merge and become one peak at 40 °C. Careful examination of line shape and line width shows the peak located at the upfield position (14.15 ppm) broadens first (Table I). Thus, this peak is most likely the A^3·T^8 pair since it is closer to the outside of the helix. The peak located at the downfield position (14.23 ppm) is assigned to the A^4·T^7 base pair, which is closer to the center of the helix. The NH–N signal located at 12.84 ppm (0–15 °C) begins to show a wider line width at 50 °C (Table I) and is therefore assigned to G^5·C^6, the center base pair of the helix.

The identities of the nonexchangeable proton resonances of the decamer have been established at high temperature. Similar assignments can also be made at low temperature by carefully following the chemical shift changes upon lowering the temperature (see next section and Figure 6). Examination of various helix base pair geometries (Kan et al., 1979) shows the H_2 of adenine is closest to the N_3H of thymine in the same Watson–Crick base pair (Figure 2). The distance is calculated to be 2.84 Å by the SEQ program (Kan et al., 1979). Because the two H_2 resonances of adenine in the decamer have been assigned (Figure 3), an NOE may be observed on the NH–N resonances of thymine when H_2 is irradiated. The results of the NOE experiment are shown in Figure 4. Only the peak at 14.06 ppm (at 20 °C) shows a negative NOE when H_2 of A^3 (Figure 3) is irradiated (the dotted spectrum in Figure 4A) (Bothner-by, 1979). The effect is clearly demonstrated by the difference spectrum shown in Figure 4B. A similar NOE experiment was applied to H_2 of A^4 (figure 3). This time, the intensity of the peak at 14.11 ppm decreased (Figure 4C). The effect was small but reproducible. No NOE is observed when T^7-H_6 is irradiated (Figure 4D). Thus, the resonances at 14.11 and 14.06 ppm are assigned to the NH–N protons of A^4·T^7 and A^3·T^8, respectively. This assignment is exactly the same as that obtained by the thermal perturbation method.

The NOE experiments were performed with a 600-MHz spectrometer located at Carnegie-Mellon University, which can only be operated at 20 °C. At this temperature, only two NH–N resonances in the G-C region of the decamer could be observed (Table I). On the basis of geometrical considerations of the helix conformation (either A or B), the NH–N of T^8 in the A^3·T^8 base pair is closest to the N_1H–N of G^9 in the C^2·G^9 pair, and the NH–N of T^7 in the A^4·T^7 base pair is closest to the NH–N of the G^5·C^6 base pair [approximately 3.6–3.7 Å, according to the computer graphic program of Kan et al. (1979)]. NOE experiments were conducted in order to assign the resonances located at 12.96 and 12.79 ppm at 20 °C (Table I). The results are shown by comparison of the peaks represented with a solid line (not irradiated) and the peaks shown with a dotted line (irradiated) in Figure 5. When the NH–N of T^8 in A^3·T^8 was irradiated, only the intensity of the resonance at 12.96 ppm was reduced (Figure 5A).

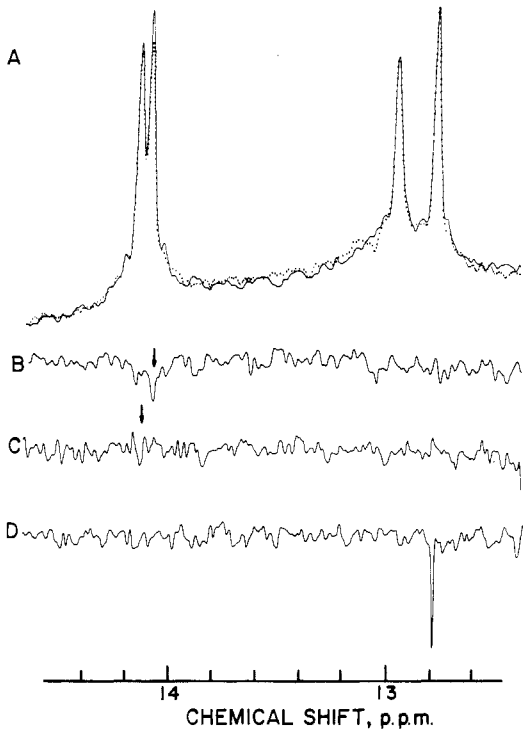

FIGURE 4: Assignment of the NH–N proton resonances of the A-T base pairs in the d-C-C-A-A-G-C-T-T-G-G helix by NOE. (A) NH–N proton resonance spectra of the d-C-C-A-A-G-C-T-T-G-G helix with an off-resonance double irradiation at 7.15 ppm (refer to Figure 3) (solid line). The dotted line represents the same region except with a double irradiation on the A^3-H_2 resonance. The NH–N C^1–G^{10} signal has already broadened to the base line. (B) Difference spectrum between the dotted and solid lines in (A). The resonance at 14.06 ppm (↓) experienced a negative NOE (Bothner-by, 1979). (C and D) These are the same as in (B) except the A^4-H_2 and T^7-H_6 signals, respectively, have been irradiated (refer to Figure 3). There is a small but recognizable negative NOE at 14.11 ppm (↓) in (C). A spike which is believed to be generated by the computer is shown at 12.8 ppm in (D).

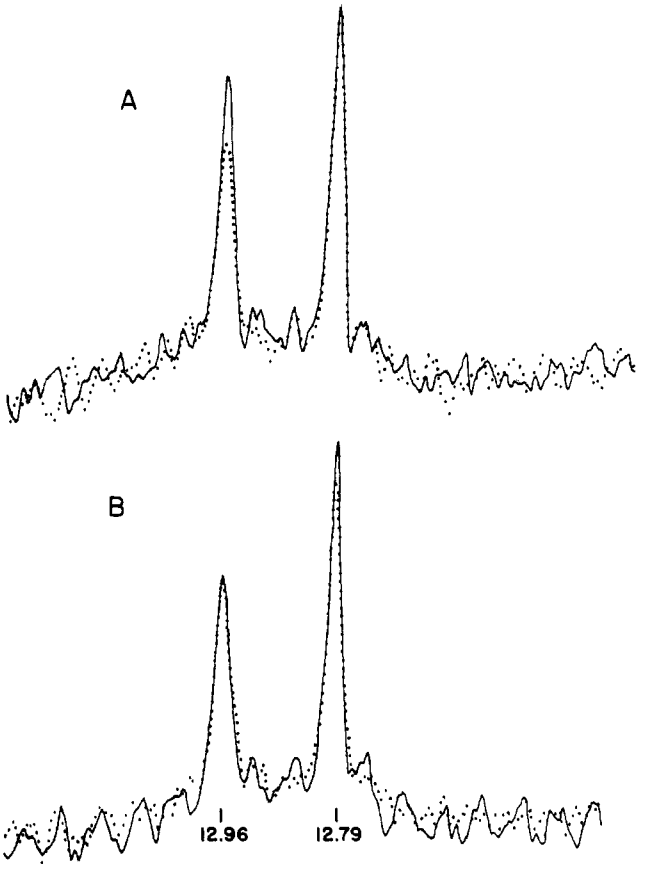

FIGURE 5: Assignment of the NH–N proton resonances of the G-C base pair in the d-C-C-A-A-G-C-T-T-G-G helix. The solid line again represents the off-resonance double irradiation, and the dotted line spectra are obtained when the irradiation frequency is set at 14.06 (A) or 14.11 ppm (B).

Similarly, when NH–N of T^7 in A^4·T^7 was irradiated, only the intensity of the resonance at 12.79 ppm was reduced. Based on these reproducible NOE observations, the resonances at 12.96 and 12.79 ppm are assigned to the NH–N proton of G^9 in the C^2·G^9 base pair and of G^5 in the G^5·C^6 base pair, respectively. The NH–N resonance of G observed at 13.24 ppm at 0 °C which disappears at 20 °C (Table I) must be the NH–N resonance of G^{10} in the outermost C^1·G^{10} base pairs of the helix.

The assignments of these base-pair NH–N resonances of the helix as derived from the NOE experiments are identical with those derived from the thermal perturbation experiment. This agreement in assignment by two independent approaches not only confirms the assignment but also confirms the assumption made in the thermal perturbation experiment; i.e., the short helix melts from the outermost base pair toward the innermost base pair.

Profiles of the Chemical Shifts of Nonexchangeable Base Protons vs. Temperature. The profiles of 17 nonexchangeable base proton resonances vs. temperature in a range from 0 to 90 °C are shown in Figure 6. Since the change in chemical shift faithfully reflects the change of the magnetic environment of each proton, this change can serve as a sensitive monitor of conformational change during helix melting. As shown in Figure 6, the chemical shift changes of each individual proton resonance are not identical. For example, H_6's of C^1 and C^2 (signals 9 and 10), H_5 of C^1 (signal 13), H_8 of A^3 (signal 2), and H_8 of G^9 (signal 7) all have very small changes over this temperature range. Since this observation implies the absence of a strong magnetic shielding center in close proximity to these protons, we can conclude that the H_8's of A^3 and G^9 are not shielded by the ring-current magnetic field of A^4 and G^{10} (Cheng et al., 1982a), respectively. This deduction implies that the base ring-current shielding effect on the base protons of the next residue is exerted by the neighboring residue on the 5′ side, and not by the neighboring residue on the 3′ side. This conclusion on the shielding effect of residues in a helical duplex is the same as that which we have previously reached for single-stranded oligonucleotides (Cheng et al., 1982a). In contrast, when the chemical shift of a proton resonance is strongly influenced by a change in temperature, this effect indicates that the proton is located in close proximity to strong magnetic shielding centers. In support of this deduction, the resonances of H_2 of A^4 (signal 3) and of H_5 of C^6 (signal 15) exhibit a large upfield shift upon helix formation. This observation indicates that H_2 of A^4 is shielded by A^3 and H_5 of C^6 is shielded by G^5 as well as A^4 in the helix. Clearly, the magnetic shielding through space is both sequence dependent and conformation dependent (Figure 6).

The profiles of the chemical shifts of the nonexchangeable protons of the equal-molar mixture of the two pentamers d-C^1-C^2-A^3-A^4-G^5 and d-C^6-T^7-T^8-G^9-G^{10} vs. temperature from 0 to 90 °C shown in Figure 7. This study confirms not only the conclusion in the preceding paragraph but also the assignment of the base proton resonances for the decamer described earlier. Upon helix formation at low temperature (Figure 7), the resonance of H_2 of A^4 (signal 3) exhibited a large upfield shift as expected for the shielding by A^3. The H_5 of C^6 (signal 15) does not exhibit any significant upfield

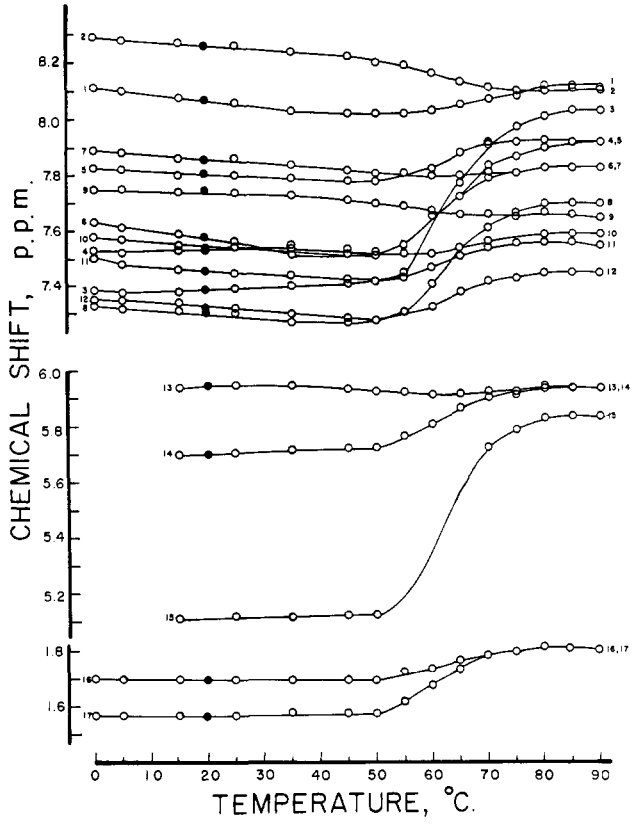

FIGURE 6: Profiles of the chemical shift data of nonexchangeable base proton resonances of d-C-C-A-A-G-C-T-T-G-G vs. temperature. The peak numbering system is the same as in Figure 1. The open circles represent data which were obtained at 360 MHz and closed circles the data obtained at 600 MHz.

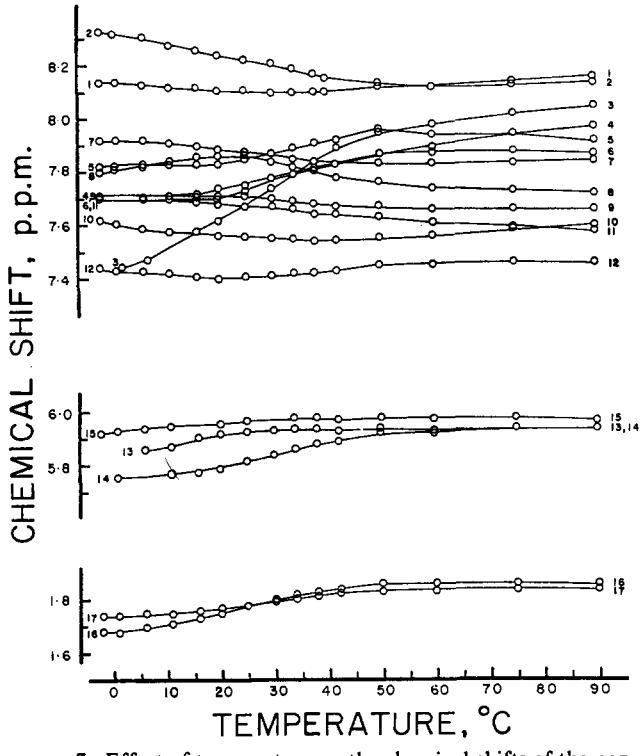

FIGURE 7: Effect of temperature on the chemical shifts of the nonexchangeable base proton resonances of 1:1 d-C-C-A-A-G/d-C-T-T-G-G mixture. All data were obtained at 360 MHz. The numbering system is the same as in Figure 1.

shift, since C^6 in the pentamer helix is located at the end of the helix. Thus, the temperature profile of the chemical shift of C^6 is similar to that of C^1, since these two residues are both

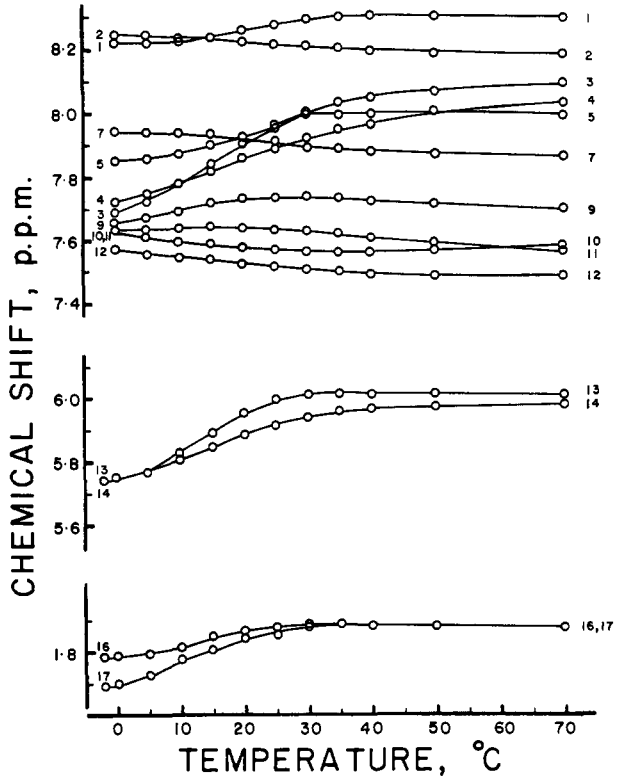

FIGURE 8: Effect of temperature on the chemical shifts of the nonexchangeable base proton resonances of 1:1 d-C-C-A-A/d-T-T-G-G mixture. All data were obtained at 360 MHz. The numbering system is the same as in Figure 1.

located at the end of the pentamer helix. It is interesting to note that upon helix formation the H_8 of G^5 (signal 6) has shifted upfield to the same extent in the pentamer helix as in the decamer helix. This occurs because the major shielding effect on G^5 is from A^4 but not from C^6 as explained above.

The second feature of Figure 6 is that half of all the profiles exhibit characteristic transition curves. The narrow breadth of the transition suggests that the helix–coil transition of the decamer can be described by a two-state model. A very stable helix is formed at the low temperature. The profiles of the nonexchangeable base proton resonances of the pentamer helix (Figure 7) and the tetramer (d-C-C-A-A + d-T-T-G-G) helix (Figure 8) all exhibit similar characteristics of a two-state model. The stabilities of the pentameric and tetrameric helices are much less than that of the decameric helix. This is indicated not only by the lower T_m values (the midpoint of the sigmoid profiles) but also by the wider breadths of the transitions. In the extreme case shown in Figure 8, the profiles never reach a low plateau even at the very low temperature (−5 °C).

As indicated from the midpoints of the sigmoidal profiles of the helix–coil transition of the decamer (Figure 6), the T_m of the outermost $C^1 \cdot G^{10}$ pair (from H_8 of G^{10}) is ~58 °C, and the T_m of the next outer $C^2 \cdot G^9$ pair (from H_5 of C^2) is ~61 °C, while T_m's of the rest of the inner base pairs (from H_2 of A^3, A^4, from H_6 of C^6, and from H_8 of G^5) are approximately 64 °C. The observed increase of T_m's from the outer base pairs to the inner base pairs strongly supports the conclusion based on the NH–N resonances that the melting of the decamer helix initiates from the outer base pairs and proceeds toward the inner base pairs.

In conclusion, the sequence dependence and conformation dependence of the temperature profiles of the nonexchangeable base protons of the helices provide valuable information for

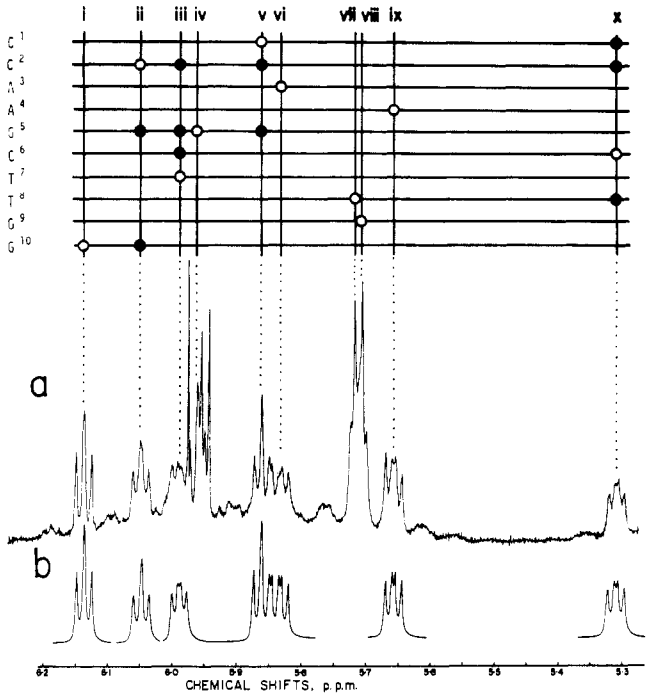

FIGURE 9: $H_{1'}$ and H_5 resonances of d-C-C-A-A-G-C-T-T-G-G in the helical state at 600 MHz (a). The computer-simulated spectra of well-resolved $H_{1'}$ resonances are shown in (b). On the top is an abacus graph designating (by circles) the changes of $H_{1'}$ corresponding to an irradiated $H_{2'}$ signal of a nucleotide in the decamer helix. The vertical lines are positions of $H_{1'}$ resonances, and the horizontal lines are the individual nucleotidyl unit of the decamer helix. The open circles designate the $H_{1'}$ signal belongs to that nucleotide, and filled circles are other $H_{1'}$ signals $H_{2'}$ or $H_{2''}$ resonances have the same chemical shift values as those of the open circles.

assignment of resonances and for studying the mechanism of the melting process.

Deoxypentose Conformation in the d-C-C-A-A-G-C-T-T-G-G Helix. The well-resolved $H_{1'}$ resonance region of this decamer helix at 20 °C obtained at 600 MHz is shown in Figure 9a. Unfortunately, the assignment of the $H_{1'}$ resonances cannot be made with certainty by using the same method used for the nonexchangeable base proton resonances, because these resonances substantially overlap in the 1:1 pentamer mixture at 20 °C (data not shown). However, the $H_{1'}$ proton resonances can be assigned through already assigned base proton resonances, i.e., H_6 of pyrimidine and H_8 of purine bases. According to the geometry of the B form of DNA, the H_8 (of purine) and H_6 (of pyrimidine) are very close to the $H_{2'}$ sugar proton in the same nucleotidyl unit. The distances are 1.9–2.2 Å in the B form. Thus, the $H_{2'}$ can be identified individually through NOE by selectively irradiating the identified H_6 or H_8 resonances. The $H_{1'}$ of the same nucleotide unit in the decamer can then be assigned by specifically decoupling the $H_{2'}$ resonance. This strategy is illustrated in Figure 10. Figure 10A shows the entire ^1H NMR spectrum of the decamer at 25 °C at 300 MHz. The $H_{2'}$ signal at 2.68 ppm receives a negative NOE when the A^3-H_8 signal is irradiated. The difference spectrum is shown in Figure 10B. The resonance of $H_{2'}$ at 2.68 ppm is now considered to be in the same nucleotidyl unit as A^3-H_8, i.e., in the A^3 unit. Then the irradiation was being carried out at 2.68 ppm, the spectral position being indicated with the downward arrow in Figure 10B. The anticipated result would be the decoupling of the $H_{1'}$ in the same A^3 unit. The region of $H_{1'}$ and H_5 resonances from Figure 10A is now expanded to be shown in Figure 10C. (In fact, the spectrum in Figure 10C and that in Figure 9A

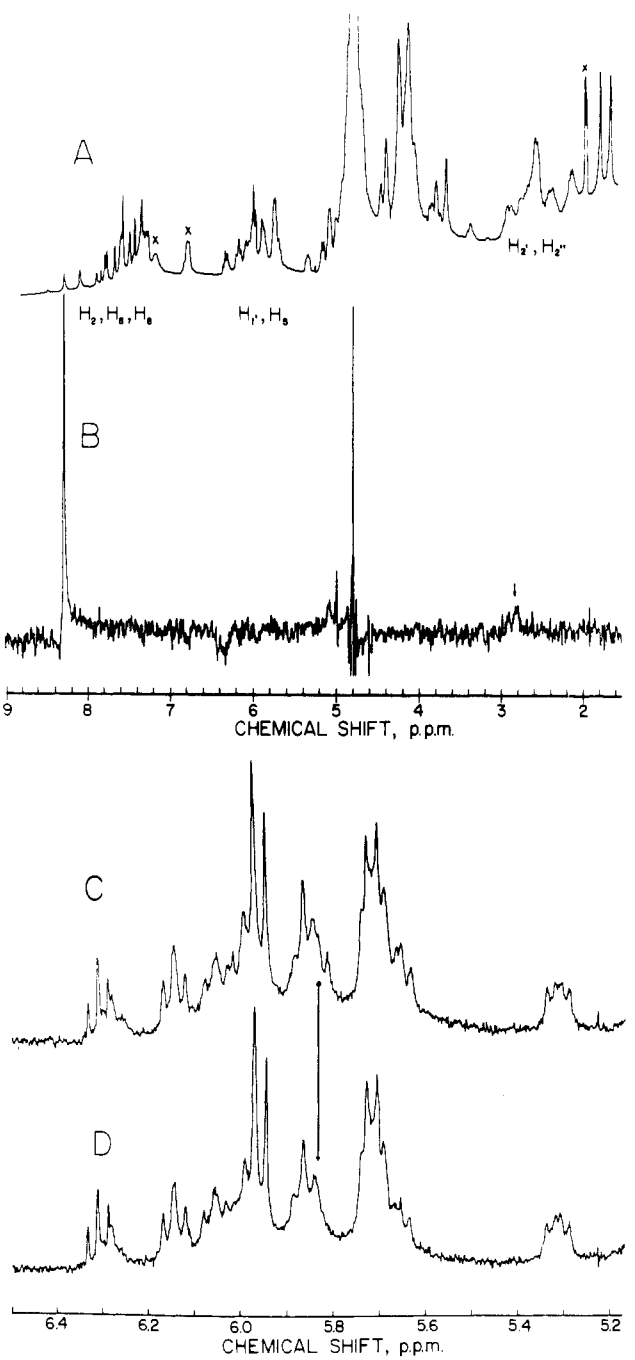

FIGURE 10: Strategy for assigning the $H_{1'}$ signals (see text). (A) Entire ^1H NMR spectrum of d-C-C-A-A-G-C-T-T-G-G at 25 °C (some impurity peaks are also shown, marked with X). (B) Difference spectrum of the decamer when A^3-H_8 is irradiated. The large peak at 8.26 ppm is caused by the applied irradiation frequency, and the small peak at 268 ppm results from NOE by the irradiation at 8.26 ppm. (C) Expanded portion of $H_{1'}$ and H_5 region of (A). (D) Same region except a weak second frequency is applied at 2.68 ppm. There is a definite change of the spectral pattern at ~5.83 ppm [designated with arrows in (C) and (D)].

contain the same set of resonances, except Figure 9 was recorded at 600 MHz and Figure 10 was recorded at 300 MHz.) Comparison of the spectrum in Figure 10C and that in Figure 10D upon irradiation at 2.68 ppm (Figure 10B) clearly shows the perturbation at the ~5.83-ppm region, which can be assigned to the $H_{1'}$ of A^3 in this $H_{2'}$–$H_{1'}$ decoupling experiment.

Because of the overlapping chemical shift values of $H_{2'}$ and $H_{2''}$ resonances from various nucleotides in the decamer (see Figure 10A), in some cases more than one $H_{1'}$ signal changes when one irradiation frequency is applied in the $H_{2'}$ region in

the $H_{2'} \rightarrow H_{1'}$ decoupling experiment. This complicates the result and makes assignment more difficult. However, in the case of d-C-C-A-A-G-C-T-T-G-G, the $H_{1'}$ signal can be resolved and assigned in the helical state. The results are shown at the top of Figure 9. The vertical lines represent the positions of $H_{1'}$ resonances (i–x), and the horizontal lines designate the bases (C^1 to G^{10}). The circles (both open and closed) indicate the perturbation of the $H_{1'}$ resonance(s) when $H_{2'}$ is irradiated. When there is more than one circle in the vertical line, this situation represents an overlapping of $H_{2'}$ resonances, therefore affecting $H_{1'}$ resonance(s) (filled circles) of other nucleotidyl unit(s) as well as the $H_{1'}$ of the same unit. As shown in Figure 9, the $H_{1'}$ resonances of A^3 (vi), A^4 (ix), T^7 (iii), and G^9 (viii) can be readily assigned because only one $H_{1'}$ changes. For the remaining six nucleotidyl units, the correct assignment (open circle) can be worked out by deduction. For example, signal x belongs to C^6 because signal iii is already assigned to T^7; in turn, signal v belongs to C^1, signal vii belongs to T^8, signal ii belongs to C^2, signal i belongs to G^{10}, and finally signal iv belongs to G^5. Thus, the $H_{1'}$ resonances of the d-C-C-A-A-G-C-T-T-G-G helix are assigned with high confidence.

The sugar conformation of an oligonucleotide can be evaluated only on the basis of $J_{1'2'}$ and $J_{1'2''}$ coupling constant data (Cheng & Sarma, 1977; Cheng et al., 1982a). The calculated $J_{1'2'}$ and $J_{1'2''}$ values obtained by computer simulation (Figure 9b) are 7.8, 7.9, 8.5, 7.3, 9.0, 9.2, and 9.6 Hz from the well-resolved multiplets i, ii, iii, v, vi, ix, and x, respectively. Thus, the percent of the $C_{2'}$-endo form of the sugar puckering is calculated as 71, 72, 77, 66, 82, 84, and 87 of G^{10}, C^2, T^7, C^1, A^3, A^4, and C^6, respectively. The result clearly shows that the percent of the $C_{2'}$-endo population increases from the terminal residue toward the inner base pair. This result indicates that the sugar conformation of this short helix is not uniform throughout and the center portion tends to resemble more of a "standard" B-DNA conformation. In summary, the sugar puckering of the decamer helix is predominantly in the $C_{2'}$-endo form ranging from 66% to 87% with an indication of a gradation which is related to conformational stability from the ends to the center of the helix.

Comparison of the Observed and Computed Values of the Helical Decameric Shifts: Conformational Dependence of the Computed Values. In view of the achievements in accurate assignment of ^1H and ^{31}p resonances of oligonucleotides and short helices (Cheng et al., 1982a,b; D. M. Cheng, L.-S. Kan, D. Frechet, P. O. P. Ts'o, S. Uesugi, T. Shida, and M. Ikehara, unpublished experiments), we now need a reliable and quantitative approach to interpret the chemical shift data. Together with the laboratory of Pullman and Giessner-Prettre, we have made several contributions in this area, particularly in conjunction with the computer graphic approach (Kan et al., 1979; Giessner-Prettre et al., 1981).

Three categories of through-space magnetic effects have been identified for theoretical and experimental investigations: (1) the ring-current anisotropic effect (RC); (2) the atomic anisotropic effect [both diamagnetic (AD) and paramagnetic (AP)]; and (3) the polarization effect of the negatively charged phosphates (POL). The first two effects have been investigated and calibrated experimentally with purine stacking in solution as a model system (Cheng et al., 1980). A mean deviation of about 0.2 ppm for eight atoms in the purine–purine dimer was obtained between the calculated and the observed values. The experimental indication of the polarization effect is currently under active investigation (D. M. Cheng et al., unpublished experiments). Due to the influence of positively charged counterions, the current calculation of this effect may be overestimated. It should be noted that quantitative evaluation of these effects can only be made with a defined conformation of nucleic acids with known coordinates.

The experimental evaluation and the theoretical calculation of the through-space magnetic effects are based on the differences in chemical shifts between the monomeric units and the corresponding unit in the dimer (the dimerization shift) or the corresponding unit in the polymer (the polymerization shift). In this study, the differences in the chemical shift of each individual residue in the monomeric form vs. its counterpart in the decamer (the decameric shift, $\Delta\delta_{10mer}$) are examined. In this calculation, it is implicitly assumed that the conformations of the residue in the monomeric form and the decameric form are the same. Therefore, the differences in chemical shifts of these atoms reflect only the influence of the nearby magnetic centers and do not contain any input from changes in the conformation of the residue from the monomeric state to the decameric state. In experimental measurements, however, the mononucleotides used for comparison purposes have a greater degree of freedom to assume a wider range of conformations than their counterparts in the decameric helix. At present, we cannot precisely evaluate the range and the population distribution of the conformation of mononucleotides in solution and the influence of conformation on chemical shifts (especially the rotation around the glycosyl C–N bond), although progress has been made in this direction both experimentally (D. M. Cheng, L.-S. Kan, P. O. P Ts'o, M. Ikehara, unpublished experiments) and theoretically (Giessner-Prettre & Pullman, 1978). In a recent study of Mitra et al. (1981 a,b), they have attempted to correct the magnetic effects of the syn population of the free monomers (especially the guanosine nucleotide), since the monomeric unit in the helix is considered to be in anti form. In their calculation, the population of $C_{2'}$ endo (or $C_{3'}$ endo) is considered to be the same in both the monomeric and helical states, and then the theoretical curves from Giessner-Prettre & Pullman (1970 a,b, 1977) were applied. These theoretical curves have not been experimentally calibrated previously, however.

Since the CD data (Miller et al., 1980) and the J values of the assigned $H_{1'}$ clearly indicate that this d-(C-C-A-A-G-C-T-T-G-G)$_2$ helix assumes a conformation close to (but not necessarily identical with) the B form, and definitely not the A or the A′ form, we may proceed to compare the observed $\Delta\delta_{10mer}$ and the computed $\Delta\delta_{10mer}$ based on the coordinates from the A′ form (Arnott et al., 1972) and the A and B forms (S. Arnott and S. Chandrasekaran, private communication).

For the base protons, Table II shows the observed decameric shifts, $\Delta\delta_{10mer}$, the computed $\Delta\delta_{10mer}$ derived from four individual contributions (RC, AD, AP, and POL), the mean deviation between the observed $\Delta\delta_{10mer}$ and the computed $\Delta\delta_{10mer}$, and finally the standard deviation of the mean deviation. For the calculation based on the B form, the mean deviation is close to the sum of RC, AD, and AP (0.20 ppm), though in general these three different approaches [i.e., RC, sum of RC, AD, and AP, and sum of RC, AD, AP, and POL (or SUM in Table II)] did not yield significantly different results (0.25 vs. 0.20 vs. 0.27). The mean deviations derived from calculations based on the B conformation are within the expected error range of 0.2 ppm and can be considered as support for the conformational assignment of this decamer based on other experimental data. As for the mean deviations based on the A and A′ conformations, the values are smallest for the RC approach (both are 0.26 ppm), become larger compared to the sum of RC, AP, and AD (0.30 and 0.41 ppm for A and A′ forms, respectively), and become the largest compared to the sum RC,

Table II: Observed and Calculated Chemical Shift Changes of All Nonexchangeable Base Proton Resonances of the d-C-C-A-A-G-C-T-T-G-G Helix[a]

proton	signal no.[b]	obsd chemical shift change (ppm)	chemical shift changes (ppm)																	
			RC			AD			AP			RC + AD + AP			POL			SUM[c]		
			A	A′	B	A	A′	B	A	A′	B	A	A′	B	A	A′	B	A	A′	B
C^1-H_5	13	0.09	−0.05	−0.04	0.04	0.00	0.00	−0.01	−0.02	−0.03	0.12	−0.07	−0.07	0.15	−0.42	−0.17	0.04	−0.49	−0.23	0.19
C^1-H_6	9	0.12	−0.04	−0.04	0.09	0.00	0.00	−0.01	−0.03	−0.04	0.13	−0.07	−0.08	0.21	−0.08	0.09	0.32	−0.14	0.01	0.53
G^{10}-H_8	5	0.33	0.61	0.62	0.15	−0.01	−0.01	−0.01	0.27	0.29	0.08	0.87	0.89	0.22	0.42	0.41	0.39	1.29	1.30	0.62
C^2-H_5	14	0.39	0.24	0.32	0.19	−0.01	−0.01	−0.01	0.30	0.34	0.26	0.53	0.66	0.44	−0.07	0.27	0.35	0.46	0.92	0.79
C^2-H_6	10	0.52	0.06	0.02	0.15	−0.00	0.00	−0.00	0.14	0.16	0.07	0.20	0.18	0.22	−0.01	0.36	0.24	0.19	0.54	0.45
G^9-H_8	7	0.27	0.17	0.17	0.08	−0.01	−0.01	−0.01	0.28	0.29	0.12	0.44	0.46	0.20	0.45	0.55	0.45	0.89	1.00	0.64
A^3-H_2	4	0.67	1.36	1.55	1.08	−0.01	−0.02	0.01	0.25	0.28	0.35	1.59	1.81	1.44	−0.01	0.06	−0.67	1.59	1.87	0.77
A^3-H_8	2	0.26	0.18	0.15	0.19	−0.01	−0.00	−0.01	0.24	0.27	0.12	0.42	0.42	0.29	0.29	0.64	0.42	0.70	1.05	0.71
T^8-H_6	12	0.51	0.06	0.05	0.06	−0.01	−0.01	−0.01	0.25	0.25	0.12	0.30	0.29	0.18	0.54	0.67	0.41	0.84	0.96	0.58
T^8-CH_3	17	0.35	0.13	0.20	0.01	−0.01	−0.02	−0.01	0.39	0.50	0.17	0.51	0.68	0.17	−0.12	−0.25	0.34	0.39	0.43	0.51
A^4-H_2	3	0.82	0.64	0.81	0.74	−0.01	−0.02	−0.00	0.26	0.30	0.31	0.89	1.10	1.04	0.02	0.08	−0.72	0.91	1.18	0.32
A^4-H_8	1	0.45	0.78	0.81	0.29	−0.01	−0.01	−0.01	0.23	0.23	0.11	0.99	1.03	0.39	0.38	0.63	0.42	1.37	1.66	0.81
T^7-H_6	11	0.31	0.17	0.13	0.06	−0.01	−0.00	−0.01	0.23	0.23	0.17	0.40	0.36	0.22	0.53	0.68	0.29	0.92	1.04	0.50
T^7-CH_3	16	0.22	0.38	0.59	0.09	−0.02	−0.02	−0.01	0.39	0.53	0.20	0.76	1.10	0.27	−0.14	−0.19	0.14	0.62	0.91	0.42
G^5-H_8	6	0.54	0.87	0.91	0.30	−0.02	−0.01	−0.02	0.24	0.24	0.17	1.10	1.14	0.45	0.40	0.57	0.44	1.50	1.71	0.89
C^6-H_5	15	0.98	0.88	1.23	0.37	−0.00	−0.00	−0.00	0.31	0.41	0.23	1.19	1.63	0.60	−0.44	−0.47	0.00	0.75	1.16	0.60
C^6-H_6	8	0.77	0.48	0.42	0.16	−0.01	−0.01	−0.01	0.20	0.18	0.16	0.67	0.59	0.32	0.45	0.60	0.24	1.12	1.19	0.56
$\bar{x}_e$[d]			0.26	0.26	0.25							0.30	0.41	0.20				0.36	0.59	0.27
S[e]			0.16	0.32	0.14							0.23	0.29	0.20				0.34	0.36	0.14

[a] The calculated values are in terms of ring-current anisotropic effects (RC), atomic anisotropic effects (diamagnetic, AD, and paramagnetic, AP), and polarization effects (POL) based on A, A′, and B DNA structures (see text). [b] Designated signal numbers, the same as in Figure 1. [c] SUM = RC + AD + AP + POL. [d] Average error of all 17 signals. [e] Standard deviations of averaged errors.

Table III: Observed and Calculated Chemical Shift Changes of NH–N Hydrogen Bonded Proton Resonances of the d-C-C-A-A-G-C-T-T-G-G Helix[a]

base pair	obsd chemical shift change (ppm)	chemical shift changes (ppm)																		
		RC			AD			AP			RC + AD + AP			POL			SUM		
		A	A′	B	A	A′	B	A	A′	B	A	A′	B	A	A′	B	A	A′	B
C^1-G^{10}	0.4	0.35	0.33	0.42	−0.02	−0.02	−0.02	0.32	0.33	0.32	0.66	0.63	0.71	−0.23	−0.11	−0.20	0.42	0.52	0.52
C^2-G^9	0.6	1.59	1.36	1.05	−0.03	−0.03	−0.03	0.61	0.55	0.41	2.17	1.88	1.43	−0.20	−0.12	−0.11	1.97	1.76	1.33
A^3-T^8	0.5	1.38	1.24	0.72	−0.01	−0.01	−0.04	0.58	0.48	0.56	1.94	1.71	1.24	0.02	0.08	−0.24	1.96	1.79	1.00
A^4-T^7	0.5	1.38	0.52	0.59	−0.03	−0.03	−0.03	0.67	0.68	0.59	1.18	1.17	1.15	−0.10	−0.09	−0.38	1.08	1.08	0.77
G^5-C^6	0.8	0.35	0.39	1.10	−0.03	−0.02	−0.04	0.61	0.67	0.63	0.93	1.04	1.70	−0.06	−0.09	0.17	0.88	0.95	1.87
$\bar{x}_e$		0.65	0.28	0.18							0.68	0.61	0.57				0.70	0.66	0.54
S		0.35	0.34	0.16							0.61	0.47	0.24				0.69	0.55	0.38

[a] Terms and conditions are the same as those in Table II.

AP, AP, and POL (0.36 and 0.59 ppm) (Table II). Since this decamer is *not* in the A or A′ form, a larger mean deviation would be expected between the observed and the computed values. Otherwise, the comparison between the observed and computed values would become better when AD and AP are added to RC. The usefulness of the POL treatment remains to be evaluated. Thus, the differences between the observed and the computed mean deviations are small for the B form in all treatments, and a detectable difference can be found among the three conformations A, A′, and B only when either RC + AD + AP or RC + AD + AP + POL values are applied.

As for the NH–N resonances, Table III shows that the agreement between the observed $\Delta\delta_{10mer}$ and the computer $\Delta\delta_{10mer}$ is excellent for the B-form calculation when only RC is used (0.18 ppm). The mean deviations for the A form (0.65 ppm) and for the A′ form (0.28 ppm) are noticeably larger. However, the mean deviation became significantly larger for all A, A′, and B conformations when AD and AP or AD, AP, and POL are added to the RC (i.e., the computation by indicated by the column labeled "RC + AD + AP" or by "SUM" in Table III). This result does not support the application of AD and AP or AD, AP, and POL currently available to the calculation of the through-space magnetic effect on NH–N protons in the helix.

Concluding Remarks

For the first time, the NH–N resonances of a DNA short helix have been assigned by both the thermal stability procedure and by NOE techniques including the use of reference to assigned base proton resonances. With all the resonances of the base protons, the $H_{1'}$ protons, and the NH–N protons individually and reliably assigned, we can use this helix as a model for the study of NMR relaxation parameters. Specifically, new techniques for assignment, including the use of time/irradiation power-dependent NOE (Hare & Reid, 1982), can be tested and calibrated for general application and for theoretical understanding.

Finally, we have begun to use the experimental NMR data on this decameric helix and the tetrametic and hexameric CG helices (D. M. Cheng et al., unpublished experiments) to compare with the theoretical computation of the through-space magnetic field effects on the base protons and NH–N protons. It is hoped that this process can bring about improvement in understanding the calculation procedure and can be extended to the sugar proton resonances.

Acknowledgments

We thank the JHU–Baltimore NMR Biomedical Research Center (established by National Institutes of Health Grant GM 27512), the Mid-Atlantic Regional NMR Facility (established by National Institutes of Health Grant P41RR00542), the California Institute of Technology, and Carnegie-Mellon University for use of the Bruker WM-300, Bruker WH-360, Bruker WM-500 (established by National Science Foundation Grant CHE79-16324), and homemade 600-MHz NMR spectrometers (supported by National Institutes of Health Grant RR00292), respectively. We also thank Dr. S. Arnott and Dr. R. E. Dickerson for providing us their unpublished coordinates and to Drs. D. H. Huang and William R. Croasmun for their technical assistance.

References

Alkema, D., Bell, R. A., Hader, P. A., & Neilson, T. (1981) *J. Am. Chem. Soc. 103*, 2866.

Arnott, S., Hukins, D. W. L., & Dover, S. D. (1972) *Biochem. Biophys. Res. Commun. 48*, 1392.

Arter, D. B., Walker, G. C., Uhlenbeck, O. C., & Schmidt, P. G. (1974) *Biochem. Biophys. Res. Commun. 61*, 1089.

Borer, P. N., Kan, L.-S., & Ts'o, P. O. P. (1975) *Biochemistry 14*, 4847.

Bothner-by, A. A. (1979) in *Biological Applications of Magnetic Resonance* (Shulman, R. G., Ed.) p 177, Academic Press, New York.

Bubienko, E., Uniack, M. A., & Borer, P. N. (1981) *Biochemistry 20*, 6987.

Cheng, D. M., & Sarma, R. H. (1977) *J. Am. Chem. Soc. 99*, 7333.

Cheng, D. M., Kan, L.-S., Ts'o, P. O. P., Giessner-Prettre, C., & Pullman, B. (1980) *J. Am. Chem. Soc. 102*, 525.

Cheng, D. M., Kan, L.-S., Leutzinger, E. E., Jayaraman, K., Miller, P. S., & Ts'o, P. O. P. (1982a) *Biochemistry 21*, 621.

Cheng, D. M., Kan, L.-S., Miller, P. S., Leutzinger, E. E., & Ts'o, P. O. P. (1982b) *Biopolymers 21*, 697.

Crawford, J. L., Kolpak, F. J., Wang, A. H.-J., Quigley, G. J., van Boom, J. H., van der Marel, G., & Rich, A. (1980) *Proc. Natl. Acad. Sci. U.S.A. 77*, 4016.

Cross, A. D., & Crothers, D. M. (1971) *Biochemistry 10*, 4015.

Dickerson, R. E., & Drew, H. R. (1981) *J. Mol. Biol. 149*, 761.

Drew, H., Takano, T., Tanaka, S., Itakura, K., & Dickerson, R. E. (1980) *Nature (London) 286*, 567.

Early, T. A., & Kearns, D. R. (1980) *Nucleic Acids Res. 8*, 5795.

Early, T. A., Olmstead, J., Kearns, D. R., & Lewis, A. G. (1978) *Nucleic Acids Res. 5*, 1955.

Giessner-Prettre, C., & Pullman, B. (1970a) *J. Theor. Biol. 27*, 87.

Giessner-Prettre, C., & Pullman, B. (1970b) *J. Theor. Biol. 27*, 341.

Giessner-Prettre, C., & Pullman, B. (1977) *J. Theor. Biol. 65*, 189.

Giessner-Prettre, C., & Pullman, B. (1978) *Nuclear Magnetic Resonance Spectroscopy in Molecular Biology* (Pullman, B., Ed.) p 161, D. Reidel Publishing Co., Dordrecht, The Netherlands.

Giessner-Prettre, C., Ribas Prado, F., Pullman, B., Kan, L.-S., Kast, J. R., & Ts'o, P. O. P. (1981) *Comput. Programs Biomed. 13*, 167.

Hare, D. R., & Reid, B. R. (1982) *Biochemistry 21*, 1835.

Hughes, D. W., Bell, R. A., England, T. E., & Neilson, T. (1978) *Can. J. Chem. 56*, 2243.

Kan, L.-S., Kast, J. R., Ts'o, D. Y., & Ts'o, P. O. P. (1979) *Comput. Programs Biomed. 10*, 16.

Miller, P. S., Cheng, D. M., Dreon, N., Jayaraman, K., Kan, L.-S., Leutzinger, E. E., Pulford, S. M., & Ts'o, P. O. P. (1980) *Biochemistry 19*, 4688.

Miller, P. S., Chandrasegaran, S., Dow, D. L., Pulford, S. M., & Kan, L.-S. (1982) *Biochemistry 21*, 5468.

Mitra, C. K., Sarma, M. H., & Sarma, R. H. (1981a) *Biochemistry 20*, 2036.

Mitra, C. K., Sarma, M. H., & Sarma, R. H. (1981b) *J. Am. Chem. Soc. 103*, 6727.

Pardi, A., Martin, F. H., & Tinoco, I., Jr. (1981) *Biochemistry 20*, 3986.

Patel, D. W. (1979) *Stereodynamics of Molecular Systems* (Sarma, R. H., Ed.) p 397, Pergamon Press, Elmsford, NY.

Patel, D. W., Kozlowski, S. A., Marky, L. A., Broka, C., Rice, J. A., Itakura, K., & Breslauer, K. (1982a) *Biochemistry 21*, 428.

Patel, D. W., Kozlowski, S. A., Marky, L. A., Rice, J. A., Broka, C., Dallas, J., Itakura, K., & Breslauer, K. (1982b) *Biochemistry 21*, 437.
Patel, D. W., Kozlowski, S. A., Marky, L. A., Rice, J. A., Broka, C., Itakura, K., & Breslauer, K. (1982c) *Biochemistry 21*, 445.
Patel, D. W., Kozlowski, S. A., Marky, L. A., Rice, J. A., Broka, C., Itakura, K., & Breslauer, K. (1982d) *Biochemistry 21*, 451.
Romaniuk, P. J., Neilson, T., Hughes, D. W., & Bell, R. A. (1978a) *Can. J. Chem. 56*, 2249.
Romaniuk, P. J., Hughes, D. W., Gregoire, R. J., Neilson, T., & Bell, R. A. (1978b) *J. Am. Chem. Soc. 100*, 3971.
Romaniuk, P. J., Hughes, D. W., Gregoire, R. J., Bell, R. A., & Neilson, T. (1979) *Biochemistry 18*, 5109.
Scheller, R. H., Dickerson, R. E., Boyer, H. W., Riggs, A. D., & Itakura, K. (1977) *Science (Washington, D.C.) 196*, 177.
Wang, A. H.-J., Quigley, G. J., Kolpak, F. J., Crawford, J. L., van Boom, J. H., van der Marel, G. & Rich, A. (1979) *Nature (London) 282*, 680.

Separation and Characterization of Products Resulting from the Reaction of *cis*-Diamminedichloroplatinum(II) with Deoxyribonucleosides†

Alan Eastman

ABSTRACT: The cancer chemotherapeutic drug *cis*-diamminedichloroplatinum(II) (*cis*-DDP) was reacted with deoxyribonucleosides, and the products were separated by high-pressure liquid chromatography and characterized by ^{1}H nuclear magnetic resonance. Monofunctional platination occurred at N(3) of cytidine, N(7) of guanosine, N(1) of adenosine, and N(7) of adenosine. Bifunctional platination occurred with guanosine N(7) to N(7), adenosine N(7) to N(7), and adenosine N(1) to N(7). In addition, mixed bifunctional products N(7) of guanosine–N(1) of adenosine and N(7) of guanosine–N(7) of adenosine were obtained. No bifunctional adducts were obtained that contained cytidine, presumably due to steric hindrance as *trans*-DDP did cross-link two cytidine residues. Similarly, no adenosine N(1) to N(1) was detected with *cis*-DDP. The only other products detected were obtained at high levels of *cis*-DDP and probably represented polymeric forms in which platinum chelates to itself.

During the past decade *cis*-diamminedichloroplatinum(II) (*cis*-DDP)[1] has been the subject of intensive investigation because of its effectiveness in treating a variety of human tumors. Much evidence supports DNA as the target molecule and that the bifunctionality of the drug is essential [reviewed in Roberts & Thomson, (1979)]. The trans isomer is chemotherapeutically ineffective even though it can also react extensively with DNA (Pascoe & Roberts, 1974; Eastman, 1982). The distance between the two chloride ligands is therefore critical and probably reflects a particular site in DNA that is accessible to the cis but not the trans compound.

Controversy still surrounds both the structure of the platinated DNA and which of the platinations are potentially most lethal to a cell. Guanine is the preferred site of reaction although a slower reaction also occurs with adenine and cytosine (Robins, 1973a,b). Various forms of bidentate chelation to a single base have been suggested as the trans isomer would be excluded from such a reaction (Mansy et al., 1973). Other evidence implicates cross-linking of adjacent guanines within the same strand of DNA as important to the mechanism of action (Kelman et al., 1972). Interstrand cross-links are also known to occur, and their formation often correlates with observed toxicity in various cell systems (Zwelling et al., 1979, 1981). However, in recent work from this laboratory, murine leukemia L1210 cells with acquired resistance to the cytotoxic action of *cis*-DDP were shown to be tolerant of much higher levels of interstrand cross-links than their sensitive parent cell line (Strandberg et al., 1982).

In all the studies so far, no satisfactory system has been reported that separates the various platinum adducts of DNA; rather, characterization has been attempted in complex mixtures. This if of particular concern in the case of deoxyadenosine where at least two positions can be platinated that potentially give rise to three bifunctional adducts. The presence of minor platinum products would also be obscured in unpurified reaction mixtures. This paper describes a system for the separation of deoxyribonucleoside-bound *cis*-DDP and their subsequent characterization as an approach to better understanding the mechanism of action of this drug.

Materials and Methods

cis-DDP and *trans*-DDP (Alfa Ventron, Danvers, MA) were dissolved in 0.02 M $NaClO_4$, pH 5.5, overnight at 37 °C. Deoxyribonucleosides (Sigma Chemical Co., St. Louis, MO) were also dissolved in 0.02 M $NaClO_4$, pH 5.5. In most experiments, *cis*-DDP at concentrations of 0.2, 1, or 5 mM was incubated at 37 °C with 1 mM deoxyribonucleoside for various time periods. The reaction products (10 μL) were then separated by HPLC on an Altex Ultrasphere ODS column (5-μm particle size; 25 × 0.4 cm) attached to a Varian Model 5000 HPLC. Elution was performed with a linear gradient of 0–30% methanol in 0.1 M aqueous ammonium acetate, pH 5.5, over 30 min at 1 mL/min and monitored with an ultraviolet (A_{254}) detector.

Reaction mixtures were scaled up in size to facilitate ^{1}H NMR. Equimolar nucleoside and *cis*-DDP (5 mM) were incubated for 24 h in the case of deoxyguanosine and deoxy-

† From the Department of Biochemistry and The Vermont Regional Cancer Center, The University of Vermont College of Medicine, Burlington, Vermont 05405. *Received August 3, 1982.* Supported by National Cancer Institute Grant CA 28599 and ACS Junior Faculty Award.

[1] Abbreviations: *cis*-DDP, *cis*-diamminedichloroplatinum(II); *trans*-DDP, *trans*-diamminedichloroplatinum(II); HPLC, high-pressure liquid chromatography; NMR, nuclear magnetic resonance.

0006-2960/82/0421-6732$01.25/0